ELSEVIER

Ceramics International 29 (2003) 619–628

CERAMICS INTERNATIONAL

www.elsevier.com/locate/ceramint

Materials synthesis and characterization of 8YSZ nanomaterials for the fabrication of electrolyte membranes in solid oxide fuel cells

Norbert H. Menzler[a,*], Dominique Lavergnat[b], Frank Tietz[a], Elena Sominski[c], Elisabeth Djurado[b], Werner Fischer[a], Guangsheng Pang[c], Aharon Gedanken[c], Hans Peter Buchkremer[a]

[a] *Forschungszentrum Jülich, Institute for Materials and Processes in Energy Systems IWV-1, 52425 Jülich, Germany*
[b] *Laboratoire d'Electrochimie et de Physico-Chimie des Matériaux et des Interfaces LEPMI, 38402 St. Martin d'Hères, France*
[c] *Bar-Ilan University, Department of Chemistry, Ramat Gan 52900, Israel*

Received 18 April 2002; received in revised form 11 September 2002; accepted 20 September 2002

Abstract

Two different nanosized materials were synthesized by two preparation methods, namely a sonochemical technique and a spray pyrolysis process. The powder properties, the sintering behavior and the resulting crystallinity with respect to their utilisation for solid oxide fuel cell electrolytes were investigated. While the spray pyrolysis provides crystallized powder without any organic residue, the sonochemical powder is amorphous with some organic residue. Crystallization begins in the 400–500 °C temperature domain. The particle sizes vary between 10 and 50 nm for the sonochemical powder and between 50 nm and 1 μm for the spray pyrolysis powder, as determined by SEM analyses. Crystal growth of both powders starts between 800 and 1000 °C. After heating and sintering at 1300 °C the resulting grain sizes of the spray pyrolysis powder are 5 times larger than those of the sonochemical powder (about 250 nm and 1.2 μm, respectively). Additionally, the maximum rate of grain growth for the spray-pyrolysed material at 97 nm/h is even higher compared with 22 nm/h for the sonochemical powder.

Keywords: D. Zirconia; Nanomaterials; SOFC; Electrolyte

1. Introduction

Due to their small particle sizes, nanomaterials offer new fields of application: they are used for enhancing the properties of commercial materials in different research fields, e.g. microtechnology, biotechnology, surface coatings for electronic devices, and also in the field of energy storage and conversion such as the development of solid oxide fuel cells (SOFCs). Some attempts have been done to lower sintering temperature [1,2], minimize component shrinkage [1–3], and achieve highly sinter-reactive ceramics [4]. Boulc'h et al. [5] successfully prepared nanostructured tetragonal zirconia ceramics with particle sizes of 300 nm containing average primary crystallite sizes of 70 nm after sintering at 1500 °C for 2 hours. Moskovits et al. [1] sintered bimodal-distributed, 4 wt.% yttria-stabilized zirconia (10–430 nm) at low temperatures (1200 °C) to enhanced densification rates. Van de Graaf et al. [4] obtained ceramics of high density and small grain sizes with YSZ (17 wt.% Y_2O_3) by heating them up to 1500 °C. They pointed out that the region between 1100 and 1200 °C, identified by abnormal grain growth, should be kept as small as possible.

Furthermore, nanomaterials may be useful for enhancing the gastightness or the ionic grain boundary conductivity [6,7] of electrolytes for SOFCs as pure material or as additive to commercially available coarser yttria-stabilized zirconia. The quality of the electrolyte layers significantly depends on the preparation procedure and on the powder properties of the single nanomaterial or as a mixture with commercial powder.

The careful characterization of both nanomaterials is the basis for the use as electrolyte material in solid oxide fuel cells. Especially informations on grain sizes, the grain growth and the rate of grain growth are necessary

---

* Corresponding author. Fax: +49-2461-612455.
E-mail address: n.h.menzler@fz-juelich.de (N.H. Menzler).

0272-8842/03/$30.00 © 2003 Elsevier Ltd and Techna S.r.l. All rights reserved.
doi:10.1016/S0272-8842(02)00209-2

to optimize the sintering parameters for gastight sintering of the electrolyte in combination with the other cell components, e.g. the substrate and the electrodes. Addtionally phase stability of the stabilzed zirconia is needed because only the cubic high-temperature form has acceptable ionic conductivity at SOFC operating temperature (750–900 °C). Thus the influence on powder characteristics of the two different synthesis methods for nano materials is investigated here. The properties of the as-prepared and thermal post-treated materials are described with respect to their use in SOFC electrolytes development. In a forthcoming publication we will report on the fabrication of electrolyte layers for SOFC applications using these powders and on the resulting properties of the sintered YSZ films.

2. Experimental

2.1. Preparation procedures

2.1.1. Tosoh powder

The commercial 8YSZ powder (8 mol% yttria-stabilized zirconia, Tosoh Company, Japan) is obtained by spray-drying (manufacturer's data) and is typically consisted of agglomerates, 50 μm in size with primary particle sizes of 200–500 nm. This powder was calcined at temperatures between 1200 and 1250 °C for 3 h. After the calcination step the material was milled in polyethylene bottles with zirconia balls (8YSZ, 3 and 5 mm, Tosoh Company, Japan) on a rolling bank for 100 h. The resulting particle sizes were in the range of 250–300 nm (d_{50}). Förthmann et al. [8] obtained cell leak-rates in the range of $10^{-4}/10^{-5}$ mbar l/s cm^2 using suspensions made with these material characteristics. This material is usually used for electrolytes in the Jülich anode-supported SOFC.

2.1.2. Nanomaterial made by the sonochemical process

The sonochemical process can be used for the production of different nanomaterials on a large scale [9–11]. The complete preparation process is described in Pang et al. [9]. Therefore only a short summary of the technology is given here.

The raw materials Y_2O_3 and $ZrO(NO_3)_2{\cdot}xH_2O$ were used for the synthesis of YSZ. Y_2O_3 was dissolved in nitric acid while the zirconyl nitrate hydrate was dissolved in deionized water. The nitric acid solution was heated to dryness. The yttrium nitrate was dissolved in deionized water and mixed with the zirconyl nitrate solution. Subsequently ammonium hydroxide was added dropwise to the suspension while applying sonication. The resulting product was centrifuged and washed with deionized water. Ethanol was added to the water-washed product and it was sonicated again for 30 min. After this step the suspension was centrifuged again. A stable solution was obtained after repeating the process of suspending the powder in ethanol and sonicating. The material was now a colloidal gel-like mass.

2.1.3. Nanomaterial made by spray pyrolysis

The spray pyrolysis process is a technology that allows powders to be produced by reactive chemical spraying from an ultrasonic atomizer. It is a cheap and easy-to-handle technique and combines synthesis methods using liquid and gaseous precursors. The resulting powders are nanosized. It is a three-step process: solution spraying, spray moving and finally spray pyrolysis. A full description of the process is given in Djurado et al. [12] while a brief description is presented here.

The precursor solutions for the synthesis were zirconyl nitrate hydrate $ZrO(NO_3)_2{\cdot}xH_2O$ (Aldrich, USA) and yttrium nitrate hydrate $Y(NO_3)_3{\cdot}4H_2O$ (Aldrich, USA). Both precursors were dissolved in distilled water. After dissolution the mixture was atomized by a high-frequency ultrasonic mist generator. By applying ultrasonication, the solution disintegrated into small drops and an aerosol was formed. The drops thus formed were of identical size and composition. The drop size is influenced by the frequency of the ultrasound and the characteristics of the initial precursor solution, e.g. precursor concentration. During the second step the aerosol is transported by a supporting gas stream to the furnace where it is dried and decomposed. Due to solvent evaporation, the system reaches a new thermodynamic equilibrium in precipitating the dissolved salts in the volume of the droplets. The products consist of fine metal oxides and the oxidation status is linked to the furnace temperature. An electrostatic filter at the outlet of the furnace collects the as-prepared nanosized dried powder. For more details please refer to [13].

Several experiments were carried out to optimize the process parameters. Table 1 gives an overview of the important parameters and the values with which the powder was synthesized.

2.2. Materials characterization

The morphology of the powders was characterized using a high-resolution scanning electron microscope equipped with a field emission gun (LEO 1530 Gemini). Thermal behavior during heating was examined by a DTA/TGA simultaneous thermal analyzer (Netzsch STA 409). The crystallization and sintering behavior

Table 1
Optimized parameters for the spray pyrolysis process

Parameter	Data
Precursor concentration of the initial solution	2.5 mol/l
Flow rate of the supporting gas	6 l/min
Vibration frequency	1.7 MHz
Furnace temperature during pyrolysis	600 °C

was studied in air by an X-ray powder diffractometer (Siemens D 5000) equipped with a high temperature chamber (Bühler HDK-S1), a diffracted beam graphite monochromator and by using Cu-K$_\alpha$ radiation. The sample powder was sedimented directly onto a heated Pt tape. The Raman spectra were recorded with a DILOR XY multichannel spectrometer and CCD detector. The green excitation line (514.53 nm) from an argon ion laser was used, the laser power was 20 mW.

3. Results and discussion

3.1. Tosoh powder

Fig. 1a and b shows SEM micrographs of the as-received powder, while in Fig. 2a and b the powder calcined at 1200 °C for 3 h is shown. In Figs. 1a and 2a an overview of the particle sizes is given, while Figs. 1b and 2b show higher magnifications of the powder surface.

The heat treatment neither changes the crystallographic cubic YSZ phase nor the agglomerate sizes are reduced, nor does significant sintering occur at this calcination temperature. Only the beginning of neck formation and particle intergrowth appear and thus an increasing agglomerate porosity was observed. After calcination the agglomerates were easier to mill due to the increased brittleness of the material.

Thermal analysis of the Tosoh powder showed no weight loss below 1200 °C and no sharp peaks were observed in differential thermal analysis (DTA).

3.2. Sonochemical powder

The particle size and the powder morphology were observed by SEM. Fig. 3 shows the micrographs of the dried material. It can be seen that the original particle size is about 10–50 nm, but the particles tend to agglomerate to highly porous structures of micromeritic scale.

Therefore a calcination step had to be included before any further experiments, because the goal of reaching higher green densities needs small particle or agglomerate sizes in addition to commercial powder (particle packing dynamics).

The thermal behavior during heating is shown in Fig. 4.

The TGA curve in Fig. 4 shows that the amount of solid in the gel-like material is about 20% indicated by the mass loss from room temperature to 100 °C, which

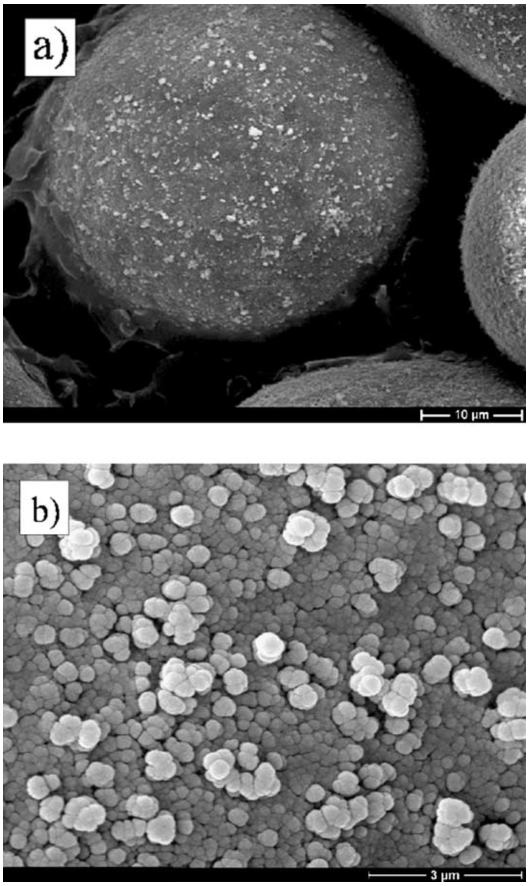

Fig. 1. SEM micrograph of the as-received Tosoh powder: (a) agglomerated particles and (b) surface of the agglomerates.

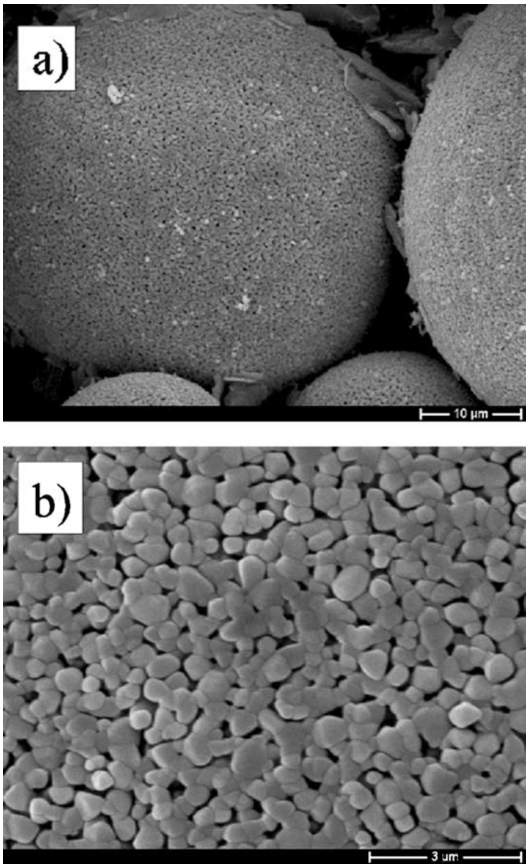

Fig. 2. SEM micrographs of the calcined commercial Tosoh powder: (a) agglomerated particles and (b) surface of the agglomerates.

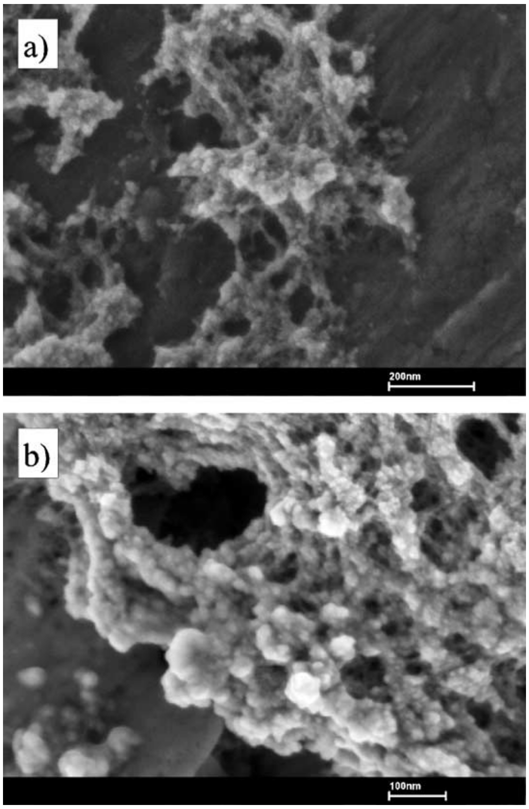

Fig. 3. SEM micrograph of the dried nanomaterial prepared by the sonochemical method: (a) and (b) (higher magnification) (note that due to the high magnification the pictures are slightly blurred).

is linked to the evaporation of ethanol. Corresponding to the mass loss, a sharp endothermal peak in the DTA signal is observed (boiling point of ethanol: 78 °C). Note that the material contains YSZ and ethanol after preparation. Above 100 °C neither significant weight loss occurs nor can peaks be observed in the DTA curve up to 1200 °C. Consequently, a drying step is needed for further processing due to the high shrinkage caused by ethanol evaporation of the as-prepared material.

The next characterization step is the examination of the crystallization behavior during sintering. Fig. 5 shows the phase evolution from room temperature up to 1200 °C measured with high-temperature X-ray diffraction. At room temperature the material is amorphous. Crystallization starts at about 400 °C indicated by the first broad peaks. During heating a simultaneous growing and narrowing of the peaks is observed due to better crystallization or enhanced grain growth. At 1200 °C the powder is well crystallized and almost single-phased. Some impurities of tetragonal phase may be present, which is indicated by a doubling of the peaks at Bragg angles higher than 60°. The Pt reflections are due to evaporation of platinum at higher temperatures from the Pt heater.

The grain size was calculated from the line broadening of five different reflections using the Scherrer formula (Fig. 6).

Fig. 6 shows that grain growth starts at 800–900 °C (no measurements below 700 °C are shown in the graph since there was no curve variation) and increases to an

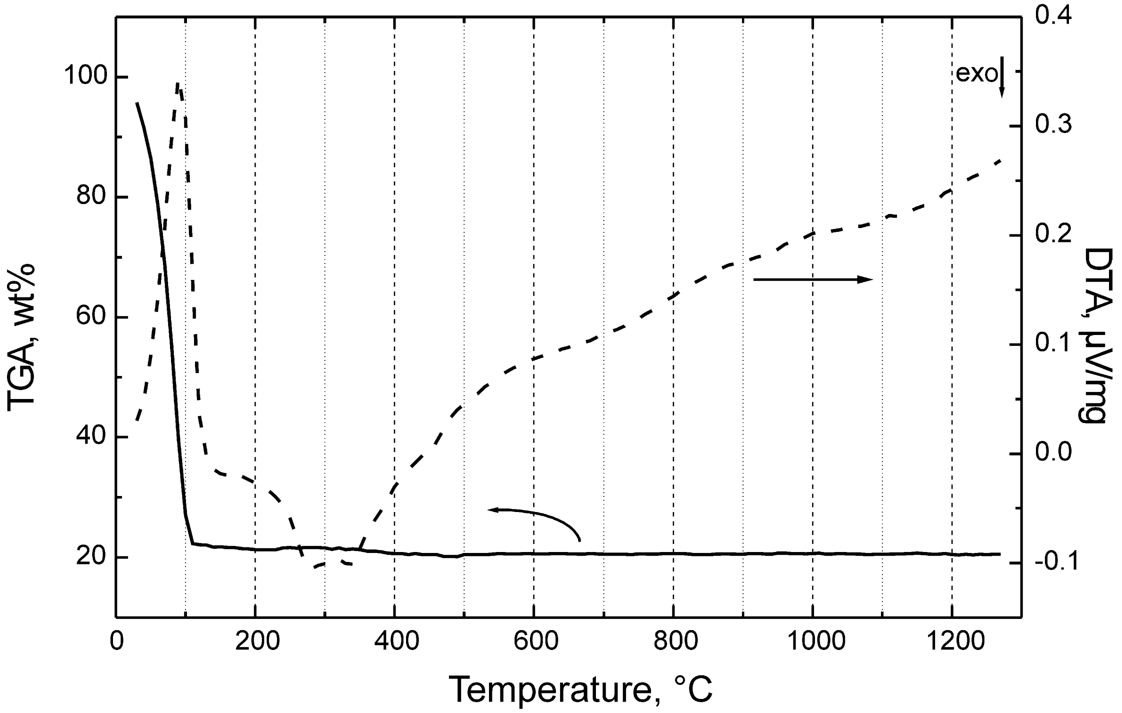

Fig. 4. TGA and DTA of the sonochemical powder.

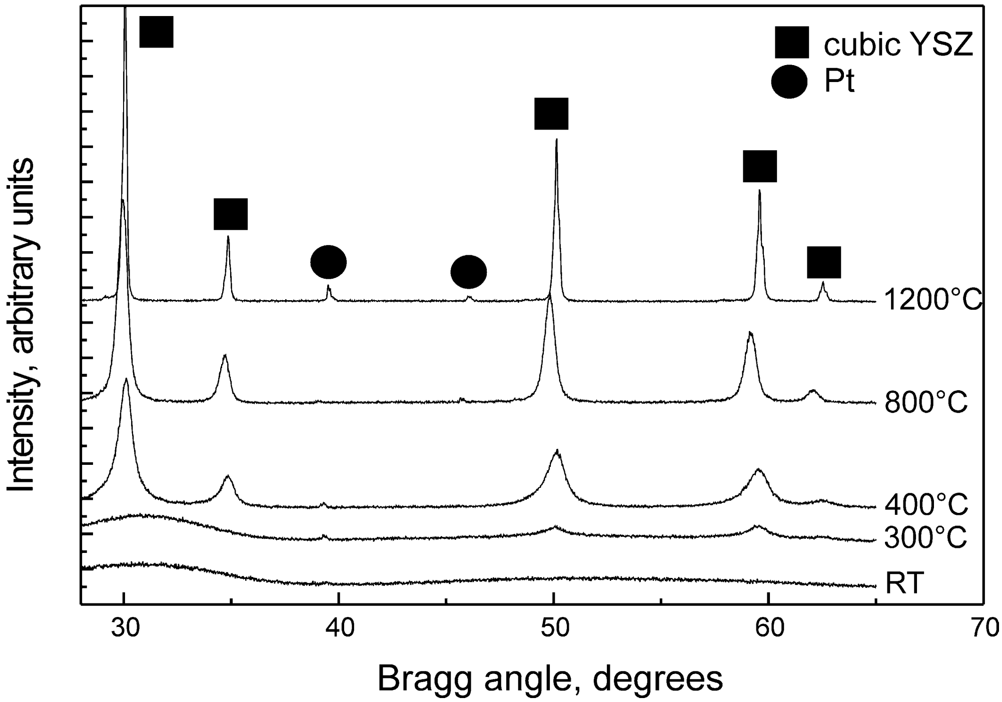

Fig. 5. HT-XRD diagram of the powder made by the sonochemical method.

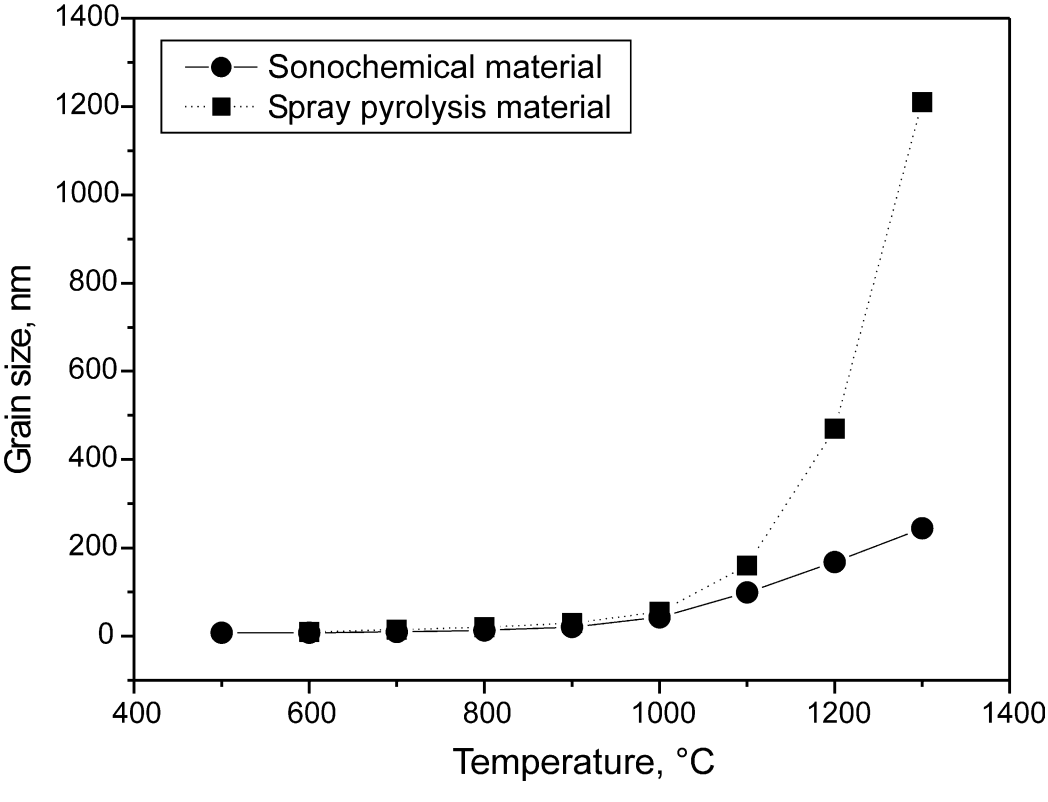

Fig. 6. Grain growth of the sonochemical (circles and solid line) and the spray pyrolysis (squares and dotted line) powder during heating.

average grain size of 250 nm during heating up to 1300 °C (medium grain growth calculated from five reflections); the growth being nearly isotropic. Isotropic growth is necessary to obtain gastight layers with no preferred growth directions. Pores or capillarity formation have to be avoided. The growth rate was calculated from the XRD data taking into account the duration of the isothermal heating step.

Fig. 7 represents the growth rate as a function of temperature.

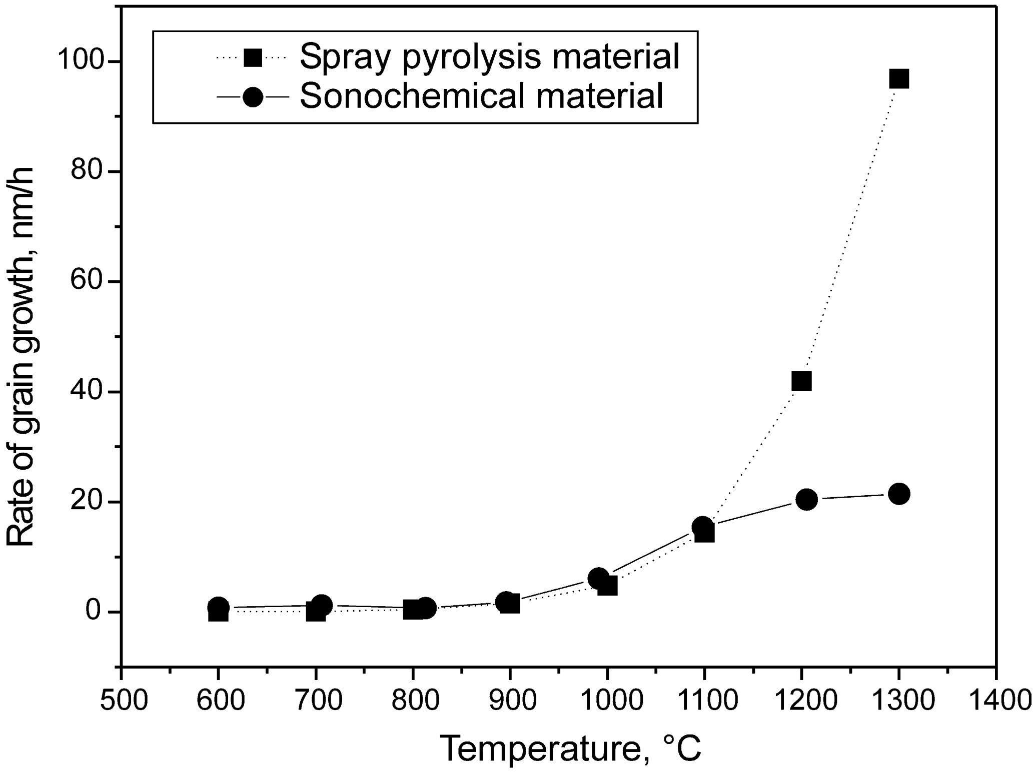

Fig. 7. Grain growth rate versus temperature for the sonochemical (circles and solid line) and the spray pyrolysis powder (squares and dotted line).

The growth rate increases rapidly between 900 °C and 1300 °C. The maximum increase of the growth rate was observed at 1050 °C. Higher temperatures lead to a decreasing slope indicating that a plateau might be reached at even higher temperatures. A growth rate of 22 nm/h is obtained at 1300 °C.

The particle sizes achieved during sintering at 1200 °C for 3.5 h in air were additionally examined by SEM and measured (Fig. 8).

The micrograph shows a well-densified material with particle sizes of mostly 250 nm in diameter. This is in good agreement with the high-temperature X-ray results of 250 nm.

Additional Raman spectra of the calcined powder (at 1000 °C) were recorded at room temperature (see Fig. 9) to confirm the XRD observation with respect to single-phased cubic yttria-stabilized zirconia. Cubic zirconia, which is the high-temperature form (phase transformations from monoclinic at room temperature to tetragonal above 1170 °C and cubic above 2280 °C) of zirconia, is required, because only the cubic form has sufficient ionic conductivity at operating temperature of SOFCs (oxygen vacancies due to integration of trivalent yttria instead of tetravalent zirconia) [14]. Monoclinic or tetragonal form have no or insufficient ionic conductivity, thus phase purity is needed.

Compared to the literature data of Yashima et al. [15], the0 obtained YSZ phase can be regarded as cubic single-phase. However, some tetragonal phase impurities, indicated by the peak shifts at 250 and 470 cm^{-1}, could not be precluded.

3.3. Spray pyrolysis powder

The powder made by the spray pyrolysis process was subjected to the same characterization steps as the sonochemical powder to compare their properties and to derive preparation property relationships.

Fig. 10 shows an SEM micrograph of the spray pyrolysis powder in the as-prepared state. In comparison to the sonochemical powder (Fig. 3), the spray pyrolysis powder consists of ideal spherical particles with a diameter between 0.05 and 1 μm. No open porosity or defects could be observed. This ideal spherical geometry is directly related to the formation of droplets using the ultrasonic atomizer.

No thermal analysis was carried out on the spray pyrolysis powder because the material is heated up to 600 °C during the production process. It can be assumed that no organic residuals remained in the powder.

High-temperature XRD patterns (Fig. 11) show broad peaks in the as-prepared spray pyrolysis powder which can be attributed to the small crystallite size of 4.8 nm as calculated from Schemer's formula. In fact, spray pyrolysis particles from 50 nm to 1 μm are polycrystalline as was previously shown by Djurado et al. [12] for tetragonal zirconia. Upon heating, the diffrac-

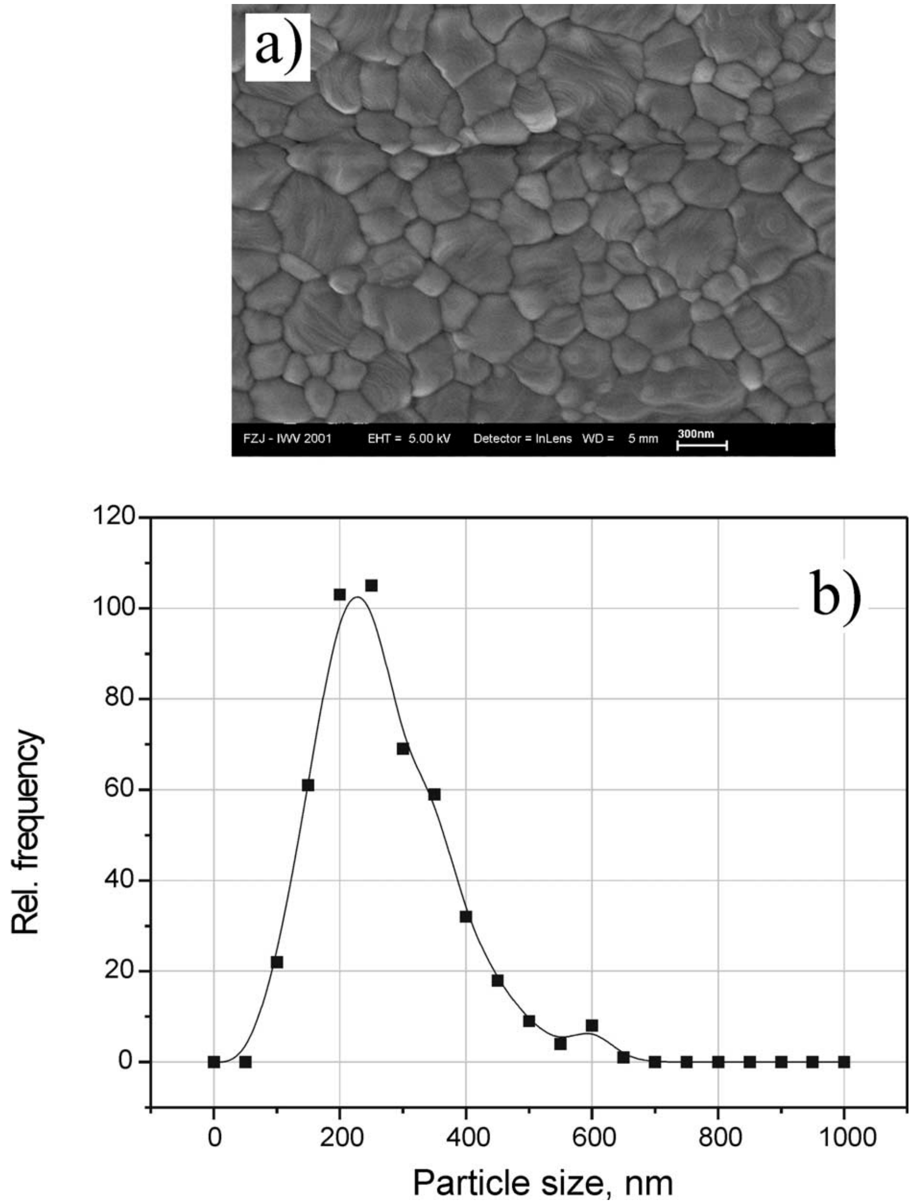

Fig. 8. SEM micrograph (a) and particle sizes (b) calculated from the SEM picture of sintered sonochemical powder (1200 °C, 3.5 h).

tion peaks became sharper indicating increasing grain growth.

This material also consisted of mostly single-phased cubic YSZ after calcination at 1200 °C. Tetragonal phase could also not be precluded, as observed for the sonochemical material.

The results of the grain growth experiment are plotted in Fig. 6. Grain growth begins at about 900 to 1000 °C and increases rapidly with increasing temperature up to 1300 °C. The particle growth is also nearly isotropic. In comparison to the sonochemical powder, whose particle growth begins at a temperature nearly 100 °C lower, the final grain sizes are significantly larger. At 1300 °C the grains were about 4–5 times larger than those of the sonochemical material.

The calculated rate of grain growth is shown in Fig. 7. The curve increases rapidly at temperatures above 1000 °C. The growth rate reached at 1300 °C was 97 nm/h. No plateau could be observed with comparison to the sonochemical material. The particle sizes obtained under identical sintering conditions are larger in spray pyrolysis powders where the growth rate is 4–5 times higher at 1300 °C than those of the sonochemical material. It is interesting to note that the polycrystalline particles present in the spray pyrolysis powder are of the same order of magnitude in diameter before and after sintering at 1300 °C.

Fig. 12 shows an SEM micrograph of an alumina substrate coated with the spray pyrolysis powder and subsequently sintered at 1300 °C for 5 h. The grain sizes

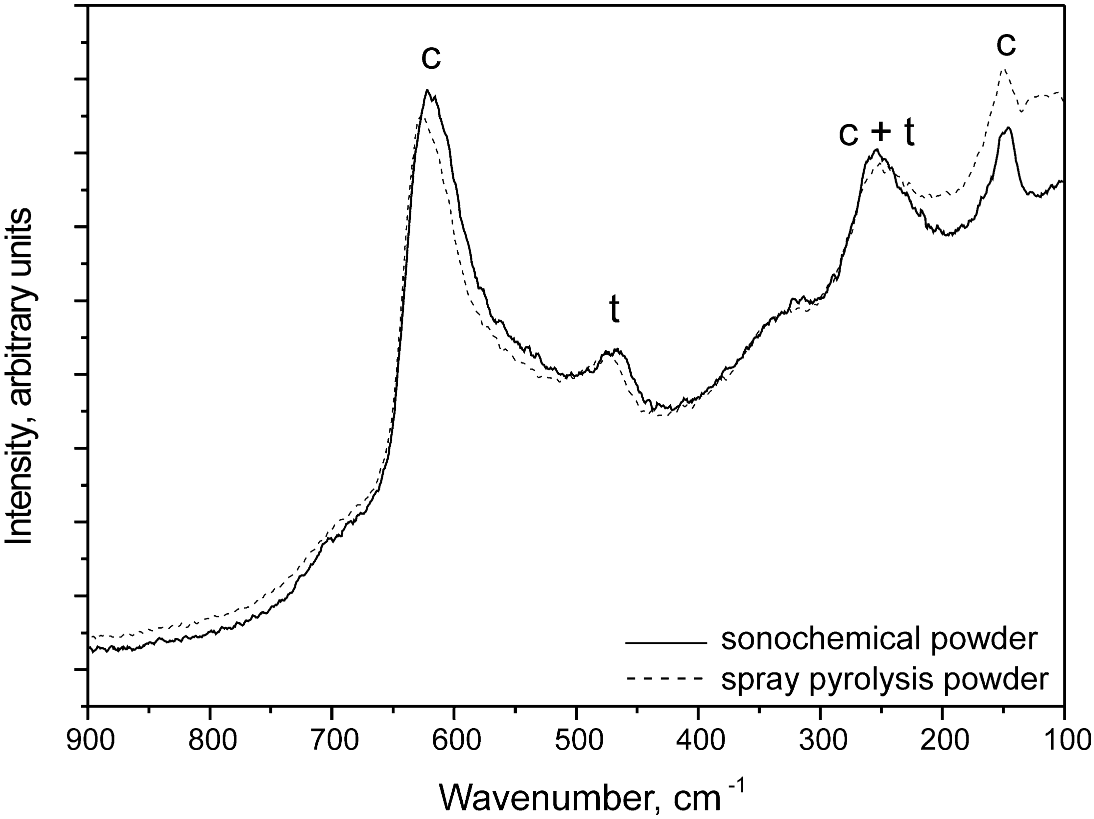

Fig. 9. Raman spectra of the sonochemical (solid line) and spray pyrolysis (dashed line) powders calcined at 1000 °C (c: cubic YSZ peaks, t: tetragonal TZP peaks).

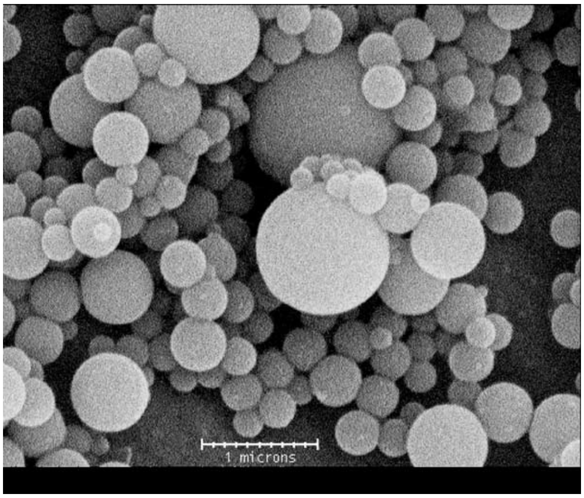

Fig. 10. SEM micrograph of the spray pyrolysis powder.

vary between 1 and 2 μm. This is in good agreement with the results obtained by high-temperature XRD (1.2 μm; Fig. 6).

The Raman spectrum of the as-prepared uncalcined powder (not shown here) shows broad and poorly developed peaks indicating small crystallites. An explanation for this result might be the difference in the particle sizes and the degree of crystallinity (the sonochemical powder is pre-calcined while the spray pyrolysis powder is not and subsequently it is only partially crystalline). Fig. 9 shows the Raman spectra of the material calcined at 1000 °C. No essential differences between the two powders can be observed.

The spray-pyrolysed material consists of particles from 50 nm to 1 μm in diameter containing nanocrystallites with an average size of 4.8 nm and is already partially crystallized after preparation. Crystallite size increases during heating and sharp reflections of mostly cubic YSZ are obtained by XRD measurements. Grain growth starts at between 900 and 1000 °C and the maximum rate of grain growth is 97 nm/h at 1300 °C. The grain size after heating at 1300 °C is about 1200 nm.

3.4. Comparison of the two nanosized powders

Due to the different preparation processes the sonochemical powder made via a wet chemical process is a gel-like material while the spray-pyrolysed material is a dry powder. Nucleation of the crystalline cubic YSZ phase has already started in the spray pyrolysis process while the sonochemical powder is amorphous. Ethanol evaporates during heating of the sonochemical material. Heating experiments show that the crystallization behavior, the grain growth and the grain growth rates varied. The sonochemical powder crystallizes at higher tem-

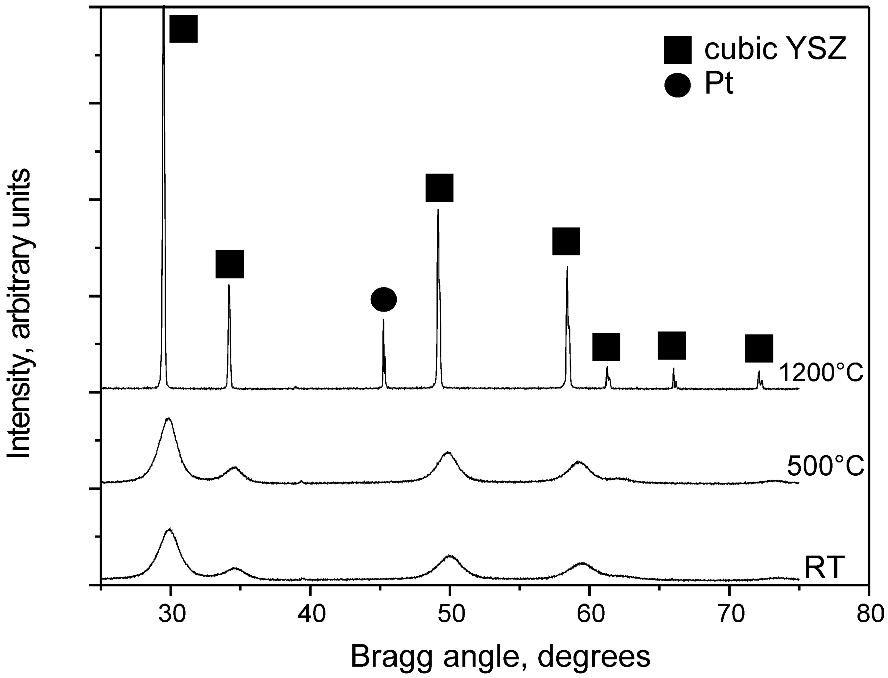

Fig. 11. HT-XRD diagram of the powder made by spray pyrolysis.

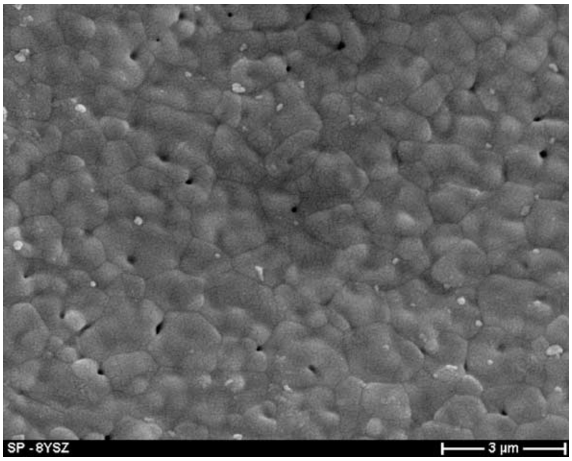

Fig. 12. SEM micrograph of the sintered spray pyrolysis powder (1300 °C, 5 h).

peratures and leads to smaller grains and lower rates of grain growth than the spray-pyrolysis one. Table 2 gives an overview of the measured parameters. In summary, the crystallite growth of the spray-pyrolysed powder begins at a higher temperature estimated to 100 °C, the grain sizes obtained were 4–5 times larger and the rate of grain growth is also 5 times higher.

Table 2
Comparison of the physical parameters of the two nanosized materials

Characterization	Sonochemical powder	Spray pyrolysis powder
Crystallization start (from XRD), °C	800–900	900–1000
Grain size after heating up to 1300 °C, nm	250	1200
Grain growth rate at 1300 °C, nm/h	22	97

4. Conclusions and outlook

Based on different preparation techniques, i.e. a wet chemical process called the sonochemical method and a physico-chemical process named the spray pyrolysis method, two nanosized powders of cubic yttria-stabilized zirconia were synthesized. The crystallization behavior and the particle growth of the two materials was characterized during heating to 1300 °C. Whereas the sonochemical powder, which is prepared in ethanol, is amorphous at room temperature and has the tendency to form agglomerates, the spray pyrolysis material is a dry, partially crystallized powder. Both materials undergo increasing crystallization during heating. Crystallization starts for the sonochemical material at 400–500 °C followd by grain growth starting at 800–900 °C. The maximum rate of grain growth is 22 nm/h at 1300 °C and the grain sizes obtained after 3.5 h at 1200 °C were 250 nm. The starting of grain growth for the spray pyrolysis powder starts in the same temperature region than that of the sonochemical powder. But the particle sizes and rates of grain growth obtained are 4-5 times higher than those for the sonochemical material (1200 nm at 1300 °C; 97 nm/h). The grain sizes measured by two different techniques (HT-XRD, SEM) are in good agreement with each other.

Ongoing work, based on these results of the characterization of the two materials, focuses on the utilisation of the nanosized powders as electrolyte material in SOFC development including coating experiments on anode-supported planar substrates with wet chemical methods, sintering experiments and gas leakage measurements.

Acknowledgements

The authors from Forschungszentrum Jülich and Bar-Ilan University are grateful to the German Federal Ministry of Education and Research (BMBF) and the Israeli Ministry of Science, Culture and Sport (MOS) for financial support under contract 0324518E, project E-1075 within the program "German-Israeli Co-operation in Energy Research". D. Lavergnat thanks Forschungszentrum Jülich and the "Region Rhône-Alpes" for financial support during his stay in Jülich.

References

[1] M. Moskovits, B.G. Ravi, R. Chaim, Sintering of bimodal Y_2O_3-stabilized zirconia powder mixtures with a nanocrystalline component, Nanostruct. Mater. 11 (2) (1999) 179–185.

[2] T. Okubo, H. Nagamoto, Low-temperature preparation of nanostructured zirconia and YSZ by sol–gel processing, J. Mater. Sci. 30 (1995) 749–757.

[3] R.J. Hellmig, H. Ferkel, Using nanoscaled powder as an additive in coarse-grained powder, J. Am. Ceram. Soc. 84 (2) (2001) 261–266.

[4] M.A.C.G. Van de Graaf, J.H.H. Ter Maat, A.J. Burggraaf, Microstructure and sintering kinetics of highly reactive ZrO_2–Y_2O_3 ceramics, J. Mater. Sci. 20 (1985) 1407–1418.

[5] E. Boulc'h, E. Djurado, L. Dessemond, J. Fouletier, Physico-chemical characterization of highly pure nanocrystalline doped TZP, J. Eur. Ceram. Soc. 21 (2001) 1847–1850.

[6] A. Cheikh, A. Madani, A. Touati, H. Boussetta, C. Monty, Ionic conductivity of zirconia based ceramics from single crystals to nanostructured polycrystals, J. Eur. Ceram. Soc. 21 (2000) 1837–1841.

[7] P. Mondal, A. Klein, W. Jaegermann, H. Hahn, Enhanced specific grain boundary conductivity in nanocrystalline Y_2O_3-stabilized zirconia, Solid State Ionics 118 (1999) 331–339.

[8] R. Förthmann, G. Blaß, H.P. Buchkremer, Deposition of thin anode and electrolyte layers for medium operation temperatures of solid oxide fuel cells, in: U. Stimming, S.C. Singhal, H. Tagawa, W. Lehnert (Eds.), Proc. 5th Int. Symp. on Solid Oxide Fuel Cells (SOFC-V), The Electrochemical Society, Pennington, NJ, USA, 1997, pp. 1003–1008.

[9] G. Pang, E. Sominska, H. Cölfen, Y. Mastai, S. Avivi, Y. Koltypin, A. Gedanken, Preparing a stable colloidal solution of hydrous YSZ by sonication, Langmuir 17 (2001) 3223–3226.

[10] Y. Wang, L. Yin, O. Palchik, Y.R. Hacohen, Y. Koltypin, A. Gedanken, Sonochemical synthesis of layered and hexagonal yttrium–zirconium oxides, Chem. Mater. 13 (2001) 1248–1251.

[11] G. Pang, S. Chen, Y. Zhu, O. Palchik, Y. Koltypin, A. Zaban, A. Gedanken, Preparation and characterization of monodispersed YSZ nanocrystals, J. Phys. Chem. B 105 (2001) 4647–4652.

[12] E. Djurado, E. Meunier, Synthesis of doped and undoped nanopowders of tetragonal polycrystalline zirconia (TPZ) by spray-pyrolysis, J. Solid State Chem. 141 (1998) 191–198.

[13] G.L. Messing, S.C. Zhang, G.V. Jayanthi, Ceramic powder synthesis by spray-pyrolysis, J. Am. Ceram. Soc. 76 (11) (1993) 2706–2726.

[14] R. Stevens, Zirconia and Zirconia Ceramics, Magnesium Elektron Ltd., 1986.

[15] M. Yashima, K. Ohtake, H. Arashi, M. Kakihana, M. Yoshimura, Determination of cubic–tetragonal phase boundary in $Zr_{1-x}Y_xO_{2-x/2}$ solid solutions by Raman spectroscopy, J. Appl. Phys. 74 (12) (1993) 7603–7605.